View Article Online
View Journal

Green Chemistry

Accepted Manuscript

This article can be cited before page numbers have been issued, to do this please use: Y. Bao, D. Zhang, M. Jia and B. Zhaorigetu, *Green Chem.*, 2015, DOI: 10.1039/C5GC02554K.

ROYAL SOCIETY OF CHEMISTRY

www.rsc.org/greenchem

View Article Online
DOI: 10.1039/C5GC02554K

Cite this: DOI: 10.1039/c0xx00000x

www.rsc.org/xxxxxx

ARTICLE TYPE

Replacing $Pd(OAc)_2$ with supported palladium nanoparticles in ortho-directed CDC reaction of alkylbenzenes

Yong-Sheng Bao,* Dongling Zhang, Meilin Jia and Bao Zhaorigetu*

Received (in XXX, XXX) Xth XXXXXXXXX 20XX, Accepted Xth XXXXXXXXX 20XX

DOI: 10.1039/b000000x

Supported palladium nanoparticles is used as an efficient catalyst for the synthesis of aromatic ketones via cross dehydrogenative coupling reactions of 2-arylpyridines with alkylbenzenes. The catalyst can be reused for five cycles without significantly losing activity. Mechanism research showed that alkylbenzene were oxidized to their corresponding aldehydes and subsequently coupled with 2-arylpyridines to generate aryl ketones through a $Pd^0/Pd^{II}/Pd^{IV}$ catalytic cycle.

Introduction

As significant materials and building blocks in the synthesis of fine chemicals, aromatic ketones have a wide range applications in many areas such as pharmaceuticals,[1] agrochemicals,[2] dyes and fragrances.[3] The direct introduction of carbonyl functional groups onto the aromatic motifs via cross dehydrogenative coupling (CDC) reaction is a more environmentally-friendly, regioselective alternative over traditional methods in aryl ketone synthesis. Many successful strategies involve Pd-catalyzed ortho-coupling reactions using aldehydes as acylation reagents.[4, 5] Compared with aldehydes, alkylbenzenes have low toxicity and are stable, commercially available, and easy to handle and thus may potentially be used as ideal acylation reagents. It is now commonly accepted that alkylbenzene could be oxidized *in situ* to give benzaldehyde in the presence of peroxide and subsequently complete various reactions, such as copper-catalyzed esterifications[6,7] and *o*-aroylations,[8] tetrabutylammonium iodide (TBAI) catalyzed synthesis of benzamides,[9] iron-catalyzed synthesis of thioesters[10] and palladium-catalyzed *ortho*-acylations[11-20] (see Scheme 1).

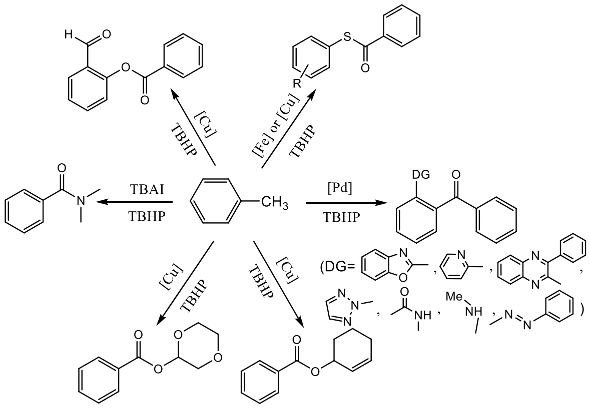

Scheme 1. Various Reactions of Toluene through Being Oxidized to Benzaldehyde Route

In 2012, B. K. Patel et al.[21] have reported $Pd(OAc)_2$ catalyzed synthesis of aromatic ketones using alkylbenzene as the aroyl moiety via directed aromatic C-H bond activation. The GC-MS analysis of the model reaction solution showed no presence of either benzaldehyde or benzyl alcohol which possibly form via a radical oxidation of toluene. They proposed that the reaction proceeded through the addition of benzyl radical to palladium substrates and the benzylic C-H bond cleavage. Whereafter, P. P. Sun et al.[14] put forward another possible mechanism, that is, toluene was oxidized to benzaldehyde and subsequently coupled with 2-arylpyridines to give the corresponding aryl ketones. So the acylation mechanism proceeding via whether the oxidative dehydrogenation of benzyl intermediate or a consecutive process that toluene is oxidized to benzaldehyde and subsequently couples with 2-arylpyridines remains to be explored and verified.

Supported palladium nanoparticles (PdNPs) has been successfully applied in many catalysis synthesis field in recent years, such as Mizoroki-Heck cross coupling reaction,[22] semihydrogenation of phenylacetylene,[23] aerobic oxidation of alcohols,[24] and directed C-H activation reactions.[25, 26] However, to the best of our knowledge, there has been no report on the supported PdNPs catalyzed *ortho*-directed CDC reaction using alkylbenzene as acyl donors.

Based on our research on the supported PdNPs catalyzed *ortho*-directed C-C coupling reaction between 2-arylpyridines and aldehydes,[27] here we verify that supported PdNPs can be used to drive the *ortho*-directed CDC reaction of alkylbenzene. In a series of supported PdNPs, $Pd/\gamma\text{-}Al_2O_3$ catalyst with a PdNPs mean diameter of 3.21 nm exhibited the best catalytic activity and it could be used five times without significant loss in catalytic

---

College of Chemistry and Environmental Science, Inner Mongolia Key Laboratory of Green catalysis, Inner Mongolia Normal University, Hohhot, 010022, China.
E-mail: sbbys197812@163.com; zrgt@imnu.edu.cn.
Tel: (+86)471-4392442

† Electronic Supplementary Information (ESI) available: Figures S1−S2, GC-MS analysis of reaction of **1a** with **2a** and **1a** with **2e**, characterization data for the products, ^1H NMR and ^{13}C NMR spectra of the products. See DOI: 10.1039/b000000x/

activity. A relatively clear mechanism was proposed based on the experimental results and relative literatures.

Experimental

Catalyst Preparation

The PdNPs on γ-Al_2O_3 and other supports were prepared by an impregnation-reduction method using the preparation of Au/γ-Al_2O_3 as reference.[28] For example, 3 wt% Pd/γ-Al_2O_3 catalyst was prepared by the following procedure: 0.97 g of γ-Al_2O_3 powder was dispersed in 50 mL of distilled water. The two kinds of aqueous solutions of $PdCl_2$ (0.01 M, 28.2 mL) and *L*-Lysine (0.03 M, 1 mL) were then added to the mixture consecutively under vigorous stirring for 20 min. Subsequently, 0.1 M NaOH aqueous solution was added into the mixture to adjust the pH to 7. An aqueous solution of $NaBH_4$ (0.35 M, 4.5 mL) was added gradually in about 10 min to the suspension. The mixture was left to stand for 24 h and the solid was separated, washed with distilled water (4 times) and ethanol (once), and dried at 80 °C. The dried solid was used directly in catalytic experiments.

Catalyst characterization

The TEM images were recorded on a JEM-2100 transmission electron microscope employing an accelerating voltage of 200 kV. The samples were suspended in ethanol and dried on holey carbon-coated Cu grids. The X-ray photoelectron spectroscopy (XPS) was recorded on a Kratos Amicus of British equipped with taper anode Mg Kα radiation. The C1s hydrocarbon peak at 284.60 eV was used as an internal standard for the correction of binding energies. The X-ray diffraction (XRD) patterns of all samples were tested on a Rigaku Ultimal IV X-ray diffractometer using Cu Kα radiation (λ=1.5406 Å) from 2θ= 10° to 80°, at a scan rate of 8° min^{-1}, with the beam voltage and beam current of 40 kV and 40 mA, respectively. The specific surface areas of all samples were obtained on a ASAP-2020 accelerated surface area and porosity analyzer of American Micromeritics Company, resulted from the nitrogen sorption data of the samples using the Brunauer-Emmett-Teller (BET) model in a relative pressure (P/P0) range between 0.06 and 0.30. The Pd content was determined by the Z-8000-type polarized Zeeman atomic absorption spectrophotometer (AAS) of Hitachi company. The Pd sensitive wavelength is 244.8 nm. The products were analyzed by GC (Shimadzu GC-2014) with a HP-5 capillary column (50 m length, 0.25 mm internal diameter, and 0.25 μm film thickness). Column, the injector and flame ionization detector temperatures were kept at 220 °C, 300 °C and 310 °C for product analysis, respectively. GC−MS analysis was detected on Thermo DSQ-II with a DB-5 column. Thin layer chromatography (TLC) was performed on pre-coated silica gel GF254 plates. The ^1H NMR and ^{13}C NMR spectra were measured on a 500 MHz Bruker Avance III nuclear magnetic resonance spectrometer, using $CDCl_3$ as the solvent with tetramethylsilane (TMS) as the internal standard. Chemical shifts (δ) are expressed in ppm. The structures of known compounds were further corroborated by comparing their ^1H NMR data with those of literature.

Activity Test

In a typical reaction, a 25 mL oven-dried reaction tube was charged with catalyst (35 mg), 2-phenylpyridine (0.2 mmol, 29 mg), tert-butyl peroxybenzoate (TBPB, 0.7 mmol, 136 mg) and toluene (2 mL). The reaction tube was placed in an oil bath at 110 °C and the reaction mixture was stirred for 24 h. The products were analyzed by GC (Shimadzu GC-2014) with a HP-5 capillary column (50 m length, 0.25 mm internal diameter, and 0.25 μm film thickness). The injector, column, and flame ionization detector temperatures were kept constantly at 300 °C, 220 °C and 310 °C, respectively. All the products were confirmed by comparison with previously reported ^1H NMR and ^{13}C NMR data.

Catalysts recycle experiment

After each reaction cycle, the reactants, solvent, and products were removed by centrifugation; the separated catalyst was washed utterly with 0.1 M NaOH ethanol solution (once), deionized water (thrice), and then washed twice with ethanol followed by centrifugal separation and drying at 80 ℃ for 10 h. The resultant catalyst was used for the next cycle.

Results and discussion

To have a good knowledge of the information for the catalyst, the fresh and used (recovered after 5th cycle) PdNPs on γ-Al_2O_3 catalysts were studied by X-ray photoelectron spectroscopy (XPS), X-ray diffraction (XRD), and transmission electron microscopy (TEM) and so on. In order to understand the state of PdNPs supported on γ-Al_2O_3, the catalysts before and after reaction were tested by XPS analysis. The XPS results of the catalysts confirm that palladium exists in the metallic state on γ-Al_2O_3 supports before and after reaction. As shown in Figure **1a**, the binding energies of Pd $3d_{5/2}$ and Pd $3d_{3/2}$ electrons are 335.11 eV and 340.36 eV of fresh catalyst and 335.02 eV and 340.27 eV of used catalyst respectively, which are identical to the bulk of palladium metal. It is shown that Pd^0 as the active center completes the catalytic cycle.

Figure **1b** depicts the XRD patterns of the fresh and used 3 wt% Pd/γ-Al_2O_3 catalysts. The XRD patterns of catalysts with different loadings (1 wt%, 5 wt%) are shown in Figure S1 (see ESI†). It is noted that no palladium peaks can be observed by XRD pattern of all samples, probably indicate that the loaded palladium did not form large particles, and was well dispersed in the support structure.

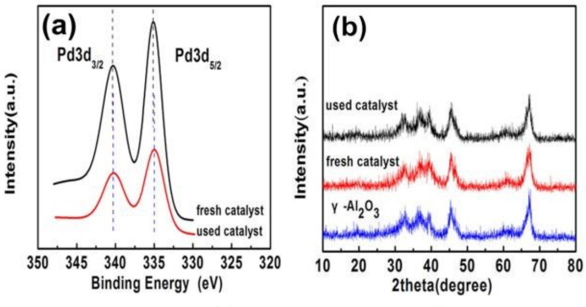

Figure 1. (a) XPS spectra of fresh and used 3 wt% Pd/γ-Al_2O_3; (b) XRD patterns of fresh and used 3 wt% Pd/γ-Al_2O_3.

View Article Online
DOI: 10.1039/C5GC02554K

The transmission electron microscopic (TEM) analysis of the fresh and used catalysts are represented in Figure **2**. The PdNPs are distributed evenly on the γ-Al_2O_3 surface, and the mean diameters of the PdNPs are 3.21 nm of fresh catalyst and 3.89 nm of used catalyst, respectively. It does not cause obvious increase in the average size of PdNPs after five runs. From the TEM images of 1 wt% and 5 wt% Pd/γ-Al_2O_3, PdNPs supported on γ-Al_2O_3 also exhibit small particles and narrow size distributions (Figure S2, see ESI†).

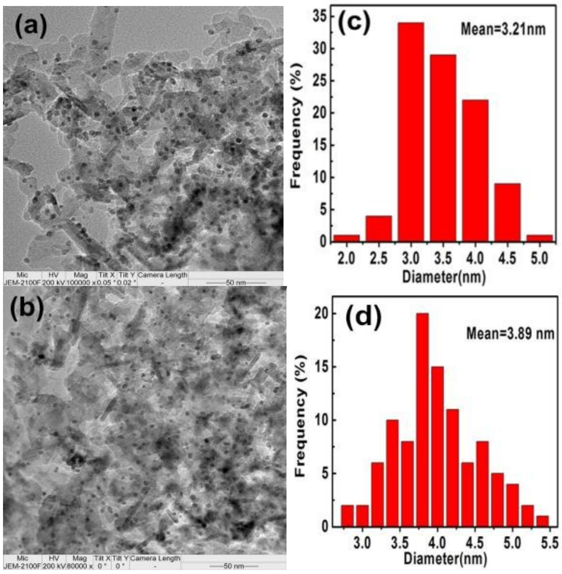

Figure 2. (a,b) TEM images of fresh 3 wt% Pd/γ-Al_2O_3 and used 3 wt% Pd/γ-Al_2O_3, respectively; (c, d) PdNPs size distributions of fresh and used catalysts, respectively.

The BET analyses were conducted and specific surface areas were given in Table **1**. Comparing the γ-Al_2O_3 with the corresponding Pd/γ-Al_2O_3 catalysts, it can be found that the surface areas of all catalysts do not arise obvious change after loading PdNPs. The amounts of Pd loading of the catalysts were derived from atomic absorption spectrophotometer (AAS), and the Pd content of fresh catalyst is approximately 3 wt %. We did note a slight decrease in Pd content after being cycled 5 times (2.86%, Table 1), which can further decrease the catalytic activity on the basis of available Pd on the support surface.

Table 1. Characterization Results of BET, AAS of Catalysts

Samples	S_{BET} (m^2/ g)	Pd loading (wt %)
γ-Al_2O_3	101	-
3 wt% Pd/γ-Al_2O_3(fresh)	114	3.02
3 wt% Pd/γ-Al_2O_3(used)	108	2.86

Our initial attempt was executed toward sp^2 C-H bond aroylation of 2-phenylpyridine **1a** using toluene **2a** as both the aroyl reagent and solvent, 3 wt% Pd/γ-Al_2O_3 as the catalyst in the presence of different oxidants such as tert-butyl hydroperoxide (TBHP), cumene hydroperoxide (CHP) and tert-butyl peroxybenzoate (TBPB). To our delight, TBPB gave the best performance (entry 4): after 24 h of refluxing in the presence of 3 wt% Pd/γ-Al_2O_3, the conversion of 2-phenylpyridine was above to 84% and the TON of this entry was 17, which was nearly 3-fold of the acylation reaction in the presence of other oxidants (entries 1-3). Besides, PdNPs supported on other oxide powders, including CeO_2 and Sm_2O_3, were prepared by the impregnation-reduction method and applied to the CDC reaction of 2-phenylpyridine with toluene (entries 5 and 6). The PdNPs on CeO_2 and Sm_2O_3 exhibited much lower activity and selectivity. The higher activity of PdNPs on γ-Al_2O_3 was for the reason that γ-Al_2O_3 had a large surface area and open porosity which could enable a high dispersion of a PdNPs catalyst.[29] We also examined the effect of different Pd loadings on the reaction. It was found that the catalytic efficiency was significantly influenced by palladium loading and that the catalyst with 3 wt % Pd exhibited the best performance. Both a decrease and increase in the reaction temperature (100 °C and 120 °C) reduced the conversion of 2-phenylpyridine (entries 9 and 10). It can be explained that TBPB might decompose at high temperature.[30] Control experiment was carried out in the absence of TBPB and it failed to give the expected product **3aa**, suggesting the importance of the oxidant (entry 11). The results for various trial reactions are summarized in Table 2.

Table 2. Optimization of reaction conditions[a]

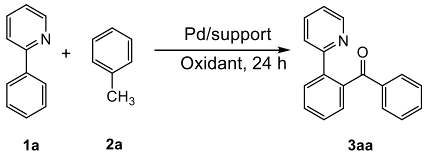

Entry	Catalyst	Oxidant	T (°C)	Conv. (%)	Sel. (%)	TON
1	3 wt% Pd/γ-Al_2O_3	TBHP 70% in water	110	26	65	5
2	3 wt% Pd/γ-Al_2O_3	CHP	110	23	49	5
3	3 wt% Pd/γ-Al_2O_3	TBHP ~5.5 M in decane	110	32	36	6
4	3 wt% Pd/γ-Al_2O_3	TBPB	110	84	97	17
5	3 wt% Pd/CeO_2	TBPB	110	46	40	9
6	3 wt% Pd/Sm_2O_3	TBPB	110	69	38	14
7	1 wt% Pd/γ-Al_2O_3	TBPB	110	68	30	14[b]
8	5 wt% Pd/γ-Al_2O_3	TBPB	110	56	56	11[c]
9	3 wt% Pd/γ-Al_2O_3	TBPB	100	70	78	14
10	3 wt% Pd/γ-Al_2O_3	TBPB	120	36	17	7
11	3 wt% Pd/γ-Al_2O_3	-	110	-	-	-

[a] Reaction conditions: **1a** (0.2 mmol), **2a** (2 mL), catalyst (35 mg), indicated oxidant (0.7 mmol), air, 24 h. Conversion and selectivity are based on **1a**, determined by GC. [b] catalyst (105 mg). [c] catalyst (21 mg).

The directed aroylation of 2-arylpyridine with a set of substituted alkylbenzenes was performed under the optimized reaction conditions, and the results are presented in Table **3**. The initial investigations were focused on the CDC reactions of 2-phenylpyridine **1a** with various alkylbenzenes **2** (entries 1-9). Various functional groups including methyl, methoxy, chloro, bromo were compatible and the desired products were achieved in moderate to good yields. For example, 4-methoxytoluene **2e** (which bears a strongly electron-donating group) afford the desired product (4-methoxyphenyl)(2-(pyridin-2-yl)phenyl)methanone **3ae** in a yield of 81% (entry 4). Gratifyingly, 4-bromotoluene **2i** and 3-bromotoluene **2j** were also reactive, even though only moderate yields of the acylation products **3ai** and **3aj**

Table 3. Substrate Scope for the Synthesis of Aromatic Ketones via C-H Functionalization[a]

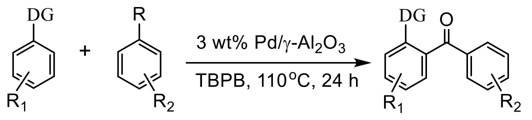

1 2 3

Entry	2-Arylpyridine	Alkylbenzene	Product	Yield[b] (%)
1	**1a**	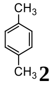 **2b**	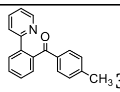 **3ab**	80
2	**1a**	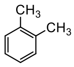 **2c**	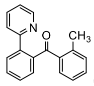 **3ac**	64
3	**1a**	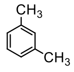 **2d**	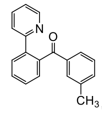 **3ad**	76
4	**1a**	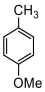 **2e**	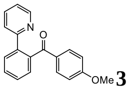 **3ae**	81
5	**1a**	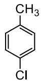 **2f**	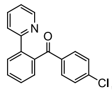 **3af**	69
6	**1a**	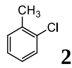 **2g**	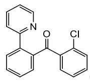 **3ag**	57
7	**1a**	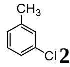 **2h**	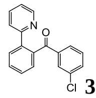 **3ah**	65
8	**1a**	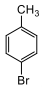 **2i**	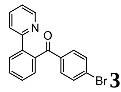 **3ai**	63
9	**1a**	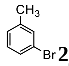 **2j**	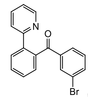 **3aj**	68
10	**1a**	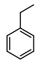 **2k**	**3aa**	31
11	**1a**	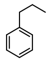 **2l**	**3aa**	44
12	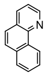 **1b**	**2a**	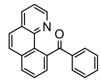 **3ba**	84
13	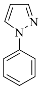 **1c**	**2a**	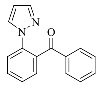 **3ca**	70
14	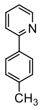 **1d**	**2a**	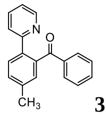 **3da**	81
15	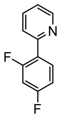 **1e**	**2a**	–	–

[a] Reaction conditions: **1** (0.2 mmol), **2** (2 mL), 3 wt% Pd/γ-Al_2O_3 (35 mg), TBPB (0.7 mmol), 110ºC, 24 h. [b] isolated yield.

were obtained (entry 8 and 9). The notable results might be explained that the aryl bromide substrates are usually very reactive in Pd^0/Pd^{II} catalytic cycles, and the bromo-substituent products can undergo further modification facilely.[4] Compared to its para or meta isomers, *o*-xylene **2c** and *o*-chlorotoluene **2g** delivered a lower yield, which resulted from the steric hindrance effect. Encouragingly, ethylbenzene and *n*-propylbenzene kept to perform this CDC reaction to give the same product as toluene respectively in 31% and 44% yields (entries 10-11). This indicated that the oxidation took place on the α-carbon of the ethylbenzene or *n*-propylbenzene and generated a small percentage of benzaldehyde.[31-33] The directly formation of benzyl radical from ethylbenzene is almost impossible because C-C homolytic cleavage is involved in the process. Therefore, the acylation mechanism proceeding via the oxidative dehydrogenation of benzyl intermediate is not accurate. In addition, the optimized reaction conditions were implemented in the coupling reactions between various phenyl-*N*-heteroarere **1** and toluene **2a** (entries 12-14). It is noted that this acylation reaction could be also applicable to heterocycle-substituted pyridines such as benzo[*h*]quinolone, and the good yield (84%) of the product benzo[*h*]quinolin-10-yl(phenyl)methanone **3ba** was obtained. The superior yield is probably due to the planar structure of benzo[*h*]quinolone.[5, 34] When 1-phenyl-1H-pyrazole **1c**, five membered nitrogen containing heterocycles served as directing- group, was employed instead of 2-phenylpyridine, the acylation reaction also proceeded expediently to afford (2-(1H-pyrazol-1-yl)phenyl) (phenyl)methanone **3ca** in 70% yield. Unfortunately, the highly electron-deficient 2-(2,4-difluoro-phenyl)pyridine **1e** failed to deliver our desired product under the present reaction conditions (entry 15). The aroylation reaction might be blocked by the electrophilic attack of the Pd(0) center to the phenyl ring.[4] It is important to point out that the reaction gave the monoacylation products selectively in all cases.

The recyclability of catalyst was examined in the reaction of 2-phenylpyridine **1a** and toluene **2a** as provided in the experimental section. As shown in Figure **3**, the catalyst can be reused for five cycles with only 13% decline of activity after the 5th recycle. Intrestingly, the average yield of five cycles of toluene was much higher than benzylaldehyde in this heterogeneous catalyzed system. From the TEM image of the used 3 wt% Pd/γ-Al_2O_3 catalyst (Figure 2b), the PdNPs still distribute evenly on the γ-Al_2O_3 surface, no apparent agglomeration was observed. The decreased catalytic activity of the PdNPs may result from the slight increase in the average size of the particles recovered after 5th cycle (Figure 2d).

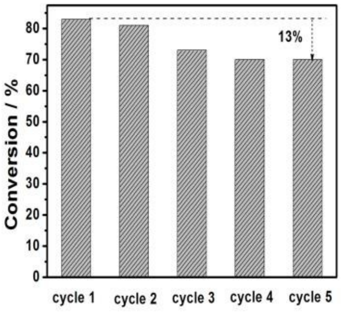

Figure 3. Recyclability of catalyst.

To gain mechanistic insight, a radical capture experiment was conducted. There was a great restraining of the reaction between 2-phenylpyridine **1a** and toluene **2a** in the presence of radical

View Article Online
DOI: 10.1039/C5GC02554K

scavenger TEMPO (0.4 mmol) and no acylation product **3aa** was detected, suggesting a possible radical approach. This result indicates that TBPB is potenially acting on both an oxidant and a radical initiator. A GC-MS analysis of the reaction solution of 2-phenylpyridine **1a** and toluene **2a** showed that both benzaldehyde and benzyl alcohol were detected which could possibly result from a radical oxidation of toluene **2a** (see ESI†). In addition, the similar result was also obtained for the reaction between 2-phenylpyridine **1a** and 4-methoxytoluene **2e** (see ESI†).

Based on the previous reports[35-41] and our own results, a tentative mechanism is illustrated in Scheme 2. First step involves the coordination of Pd^0 with the nitrogen atom of the pyridine group of 2-phenylpyridine **1** and the further oxidation of Pd^0 to Pd^{II} by air.[42] Subsequently Pd^{II} activates the *ortho* C-H bond through chelate-directed effect to afford palladacycle intermediate **A**. Secondly, the reaction of TBPB with benzaldehyde which is resulted from the oxidation of toluene **2** provides a benzoyl radical by releasing the *tert*-butyl alcohol (or benzoic acid). And intermediate **A** coordinated with benzoyl radical and benzoate radical to form an Pd^{IV} complex **B**,[43, 44] which fast releasing benzoic acid to form intermediate **C**. Finally, the final product **3** is generated through the reductive elimination of intermediate **C** and releases a Pd^0 to continue catalytic cycle.

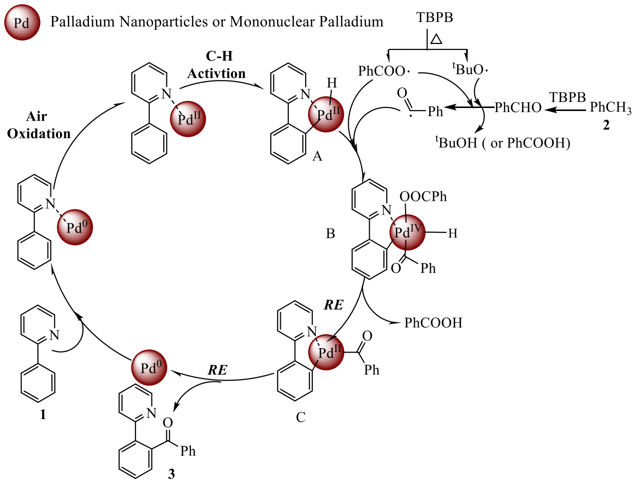

Scheme 2. Possible reaction mechanism

Conclusions

In summary, it is found for the first time that metallic state palladium, Pd^0, can catalyze the *ortho*-directed CDC reaction of alkylbenzenes including methyl, ethyl and propyl benzene for the synthesis of aromatic ketones via a $Pd^0/Pd^{II}/Pd^{IV}$ catalytic cycle. Differed from B. K. Patel's report, the acylation reaction might undergo through another possible mechanism, that is, the alkylbenzenes were oxidized to their corresponding aldehydes and subsequently coupled with 2-arylpyridines to generate aryl ketones. Using supported PdNPs as heterogeneous catalyst, TBPB as the oxidant, various methylarenes which bear both electron-withdrawing and electron-donating groups, can react with 2-arylpyridine to synthesize the corresponding ketones in yields up to 84%. The catalyst can be readily recovered and reused for five cycles with only 13% decline of activity after the 5th recycle. The practicality of this study may inspire further studies on the heterogeneous catalyzed *ortho*-directed acylation reactions. With the advantages of easy separation, recycling of heterogeneous catalyst and high catalytic activity, the PdNPs catalyst would be an alternative to $Pd(OAc)_2$ in more catalytic organic reaction.

Acknowledgements

This research was financially supported by National Science Foundation of China (21462031) and the Initial Special Research for 973 Program (2014CB460609).

Notes and references

1 P. J. Harrington, E. Lodewijk,. *Org. Process Res. Dev.* 1997, **1**, 72-76.
2 S. Gmouh, H. L. Yang, M. Vaultier, *Org. Lett.* 2003, **5**, 2219-2222.
3 H. Surburg, J. Panten, Wiley-VCH: Weinheim, 2006.
4 X. F. Jia, S. H. Zhang, W. H. Wang, F. Luo, J. Cheng, *Org. Lett.* 2009, **11**, 3120-3123.
5 O. Baslé, J. Bidange, Q. Shuai, C. J. Li, *Adv. Synth. Catal.* 2010, **352**, 1145-1149.
6 W. Ali, S. Guin, S. K. Rout, A. Gogoi, B. K. Patel, *Adv. Synth. Catal.* 2014, **356**, 3099-3105.
7 S. K. Rout, S. Guin, W. Ali, A. Gogoi, B. K. Patel, *Org. Lett.* 2014, **16**, 3086-3089.
8 S. K. Rout, S. Guin, A. Banerjee, N. Khatun, A. Gogoi, B. K. Patel, *Org. Lett.* 2013, **15**, 4106-4109.
9 J. B. Feng, D. Wei, J. L. Gong, X. X. Qi, X. F. Wu, *Tetrahedron Lett.* 2014, **55**, 5082-5084.
10 J. Feng, G. P. Lu, C. Cai, *RSC Adv.* 2014, **4**, 54409-54415.
11 Y. Zheng, W. B. Song, S. W. Zhang, L. J. Xuan, *Tetrahedron* 2015, **71**, 1574-1580.
12 P. He, Q. S. Tian, C. X. Kuang, *Synthesis* 2015, ***47***, 1309-1316.
13 S. K. Santra, A. Banerjee, B. K. Patel, *Tetrahedron* 2014, **70**, 2422-2430.
14 Z. P. Xu, B. Xiang, P. P. Sun, *RSC Adv.* 2013, **3**, 1679-1682.
15 Y. N. Wu, P. Y. Choy, F. Mao, F. Y. Kwong, *Chem. Commun.* 2013, **49,** 689-691.
16 Y. N. Wu, L.- J. Feng, X. Lu, F. Y. Kwong, H. B. Luo, *Chem. Commun.* 2014, **50**, 15352-15354.
17 H. Y. Song, D. Chen, C. Pi, X. L. Cui, Y. J. Wu, *J. Org. Chem.* 2014, **79**, 2955-2962.
18 Z. W. Yin, P. P. Sun, *J. Org. Chem.* 2012, **77**, 11339-11344.
19 F. Xiong, C. Qian, D. E. Lin, W. Zeng, X. X. Lu, *Org. Lett.* 2013, **15**, 5444-5447.
20 J. Q. Weng, Z. Q. Yu, X. H. Liu, G. F. Zhang, *Tetrahedron Lett.* 2013, **54**, 1205-1207.
21 S. Guin, S. K. Rout, A. Banerjee, S. Nandi, B. K. Patel, *Org. Lett.* 2012, **14**, 5294-5297.
22 P. Puthiaraja, K. Pitchumani, *Green Chem.* 2014, **16**, 4223-4233.
23 D. S. Deng, Y. Yang, Y. T. Gong, Y. Li, X. Xu, Y. Wang, *Green Chem.* 2013, **15**, 2525-2531.
24 J. Chen, Q. H. Zhang, Y. Wang, H. L. Wan, *Adv. Synth. Catal.* 2008, **350**, 453-464.
25 S. Korwar, K. Brinkley, A. R. Siamaki, B. F. Gupton, K. C. Ellis, *Org. Lett.* 2015, **17**, 1782-1785.
26 A. J. Reay, I. J. S. Fairlamb, *Chem. Commun.*, 2015, **51**, 16289—16307.
27 D. Zhang, B. Zhaorigetu, Y. S. Bao, *J. Phys. Chem. C* 2015, **119**, 20426−20432.
28 Y. L. Zhang, Q. Xiao, Y. S. Bao, Y. J. Zhang, S. Bottle, S. Sarina, B. Zhaorigetu, H. Y. Zhu, *J. Phys. Chem. C* 2014, **118**, 19062-19069.
29 Y. Rozita, R. Brydson, T. P. Comyn, A. J. Scott, C. Hammond, A. Brown, S. Chauruka, A. Hassanpour, N. P. Young, A. I. Kirkland, *ChemCatChem* 2013, **5**, 2695-2706.

30 T. He, H. J. Li, P. H. Lia, L. Wang, *Chem. Commun.*, 2011, **47**, 8946-8948.

31 M. Arshadi, M. Ghiaci, *Appl. Cata. A: Gen.* 2011, **75**, 399.

32 K. N. Bhagya, V. Gayathri, *J Porous Mater* 2012, **19**, 1037–1045.

33 B. Du, B. Jina, P. Sun, Org. Biomol. Chem., 2014, **12**, 4586-4589.

34 A. R. Dick, M. S. Remy, J. W. Kampf, M. S. Sanford, *Organometallics* 2007, **26**, 1365-1370.

35 X. Chen, K. M. Engle, D. H. Wang, J. Q. Yu, *Angew. Chem., Int. Ed.* 2009, **48**, 5094-5115.

36 M. Catellani, F. Frignani, A. Rangoni, *Angew. Chem. Int. Ed. Engl.* 1997, **36**, 119-122.

37 D. Alberico, M. E. Scott, M. Lautens, *Chem. Rev.* 2007, **107**, 174-238.

38 D. J. Cárdenas, B. M. Matute, A. M. Echavarren, *J. Am. Chem. Soc.* 2006, **128**, 5033-5040.

39 B. Mariampillai, J. Alliot, M. Z. Li, M. A. Lautens, *J. Am. Chem. Soc.* 2007, **129**, 15372-15379.

40 P. Mauleón, I. Alonso, J. C. Carretero, *Angew. Chem. Int. Ed.* 2001, **40**, 1921-1923.

41 K. M. Gericke, D. I. Chai, N. Bieler, M. Lautens, *Angew. Chem.* 2009, **121**, 1475-1479.

42 Y. J. Liu, H. Xu, W. J. Kong, M. Shang, H. X. Dai, J. Q. Yu, *Nature*, 2014, **515**, 389-393.

43 F. J. Hernández, A. Arcas, J. Vicente, *Chem. Eur. J.* 2012, **18**, 7780-7786

44 J. Vicente, A. Arcas, F. J. Hernández, D. Bautista, *Angew. Chem., Int. Ed. Engl.* 2011, **50**, 6896-6899.

View Article Online
DOI: 10.1039/C5GC02554K

Pd(0) = Supported palladium nanoparticles

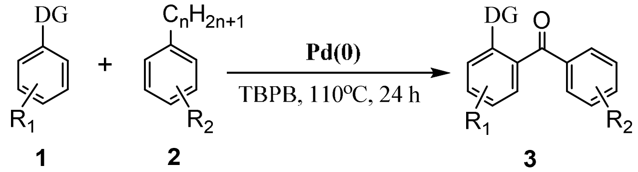

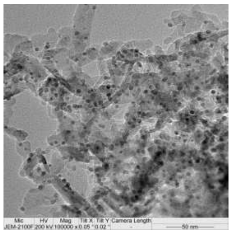

TEM images

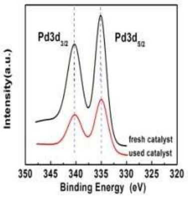

XPS spectra

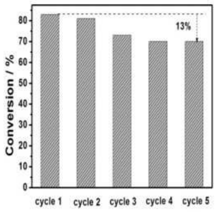

Recyclability of the Catalyst